A novel multi-resonant and wideband fractal antenna for telecommunication applications

Ibrahime Hassan Nejdi[1], Youssef Rhazi[1], Mustapha Ait Lafkih[1], Seddik Bri[2], Lamsalli Mohammed[3]
[1]Laboratory of Automatics, Energy Conversion and Microelectronics (LACEM), Faculty of Sciences and Technology, Sultan Moulay Slimane University, Beni-Mellal, Morocco
[2]Material and Instrumentations Group, Electrical Engineering Department, Superior School of Technology, Moulay Ismail University, Meknes, Morocco
[3]Information System and Telecommunication Laboratory, Faculty of Sciences, Abdelmalek Essaadi University, Tetouan, Morocco

Article Info

Article history:

Received Jun 24, 2021
Revised Mar 20, 2022
Accepted Apr 6, 2022

Keywords:

Circular antenna
Fractal antenna
Manufactured antenna
Multiband antenna
Worldwide interoperability for microwave access

ABSTRACT

This letter presents the design, simulation, and measurement of a novel multiband fractal circular antenna for wireless applications. In the antenna design, we used a circular antenna where we took a ring. Then, in the first iteration, we added a new ring divided into two of the same size. For the second iteration, we added a ring of the same size after dividing it into two halves. In the third iteration, we added the third ring of the same size after dividing it into four. Due to the resonator defection, we were able to reduce the size of the starting antenna from 60×70×2 mm^3 to 50×50×1.6 mm^3, to get the frequency of 2.48 GHz, and we generated new bandwidths with a high gain that reaches 5.02 dB. The proposed antenna radiation characteristics, such as the impedance matching, the gain, the radiation pattern, and the surface current distribution are presented and discussed. We find that the simulated and measured results are in acceptable agreement and affirm the good performance of the proposed antenna. The results obtained affirm that the proposed fractal antenna is a better candidate for integration into wireless communication circuits.

Corresponding Author:

Ibrahime Hassan Nejdi
Laboratory of Automatics, Energy Conversion and Microelectronics (LACEM), Faculty of Sciences and Technology, Sultan Moulay Slimane University
Beni-Mellal, Morocco
Email: nejdi.ibrahime.hassan@gmail.com

1. INTRODUCTION

At present, in view of communication technologies progress, there is an increasing demand for miniature antennas with multiband and/or wideband operations and which have great radiation efficiency. In the literature, we find various methods to generate multiband operations to respond to development requirements [1-19]. Numerous techniques are suggested to generate multiband and/or wideband operations to cover wireless local area network (WLAN), worldwide interoperability for microwave access (WiMAX), and C band applications [1]–[4]. Fractal antennas are one of the methods that allows miniaturizing and providing a multiband and/or wideband characteristic at low cost, as these patches perfect the input impedance matching. To cover the band 1.64-1.94 GHz, Zhong and the the other authors in [5] present a bow-tie patch antenna. Various fractal antenna methods (Sierpinski, Koch, Minkowski and Hilbert) are proposed in the literature for multiband operation [6]–[10]. A modified Sierpinski joint fractal antenna is presented in [6] for c-band and X-band applications. To design a wideband antenna, Nsir *et al.* [8] adopted the fractal Koch antenna and introduced a slot inside the patch to cover global system for mobile (GSM), universal mobile telecommunication system (UMTS), wireless local area network (WLAN), and long-term evolution (LTE). However, fractal antennas with a self-affinity and self-similitude structure are one of the methods that allow antennas to be miniaturized and provide a multiband characteristic [11], [12]. It also proves to be one of the best techniques for having a compact and multiband patch antenna. In [13]–[16] presented different forms of spiral structure geometry. Benavides *et al.* [13] incorporated these spiral antennas into a faulty ground plane where they intentionally modified the ground plane to increase antenna performance such as gain and bandwidth.

A novel multiband monopole fractal antenna with a compact size is presented in this paper. For the proposed antenna design, we welded two half rings onto the main ring in the first iteration. Then, in the second iteration, we added the second ring with the same diameter as the main ring after dividing it into two halves, and finally, we added four quarter rings in the last iteration. The proposed antenna can thus operate in three frequency bands between 2 and 6 GHz to cover WiMAX, WLAN, and C band, with wide bandwidth and excellent radiation characteristics. We designed, simulated, and optimized the antenna using the commercial electromagnetic wave (EM) simulator Ansys heart failure survival score (HFSS), and validated the results with CST studio. After manufacturing the optimized antenna, we tested it with the vector network analyzer augmented and virtual reality (AVR) Rohde and Schwarz ZVB20.

The suggested three-band fractal antenna is presented in section 2, along with its final dimensions. This section explains the various procedures involved in obtaining the final antenna, as well as an evolution comparison of the bandwidth, adaptability, and gain. The fabricated antenna is shown in section 3, along with a synthesis of the results obtained and a table comparing the results to those found in the literature.

2. ANTENNA DESIGN

Figures 1(a) and 1(b) present the top and bottom view of the proposed antenna. The patch is fed by a 50 Ω microstrip line fabricated on an FR4 substrate with a dielectric constant of 4.4 and a size of 50×50×1.6 mm^3. On the other side of the substrate, we engraved the ground plane. We propose in this work an antenna geometry based on a self-repeating geometric. For the patch design, Figure 2 depicts the proposed fractal antenna geometry step configuration. We extracted a ring from the initiator circular antenna. Then, we soldered a ring of the same diameter as the main ring after dividing it into two to create the first iteration shown in Figure 2(a). Similarly, in the second iteration, we added a second ring divided into two, which we displayed in Figure 2(b). We added in the third iteration, the third ring divided into four, as shown in Figure 2(c). We note that the three rings added in the three iterations have the same dimensions as the main ring. To have a well-matched response, two rectangular slots of width "eg" are etched on the ground plane. By adopting this configuration, we have been able to reduce the size of the starting circular antenna and increase the number of resonant frequencies between 2 and 6 GHz with excellent radiation characteristics. The proposed antenna was manufactured with all design parameters. Table 1 presents the ultimate dimensions.

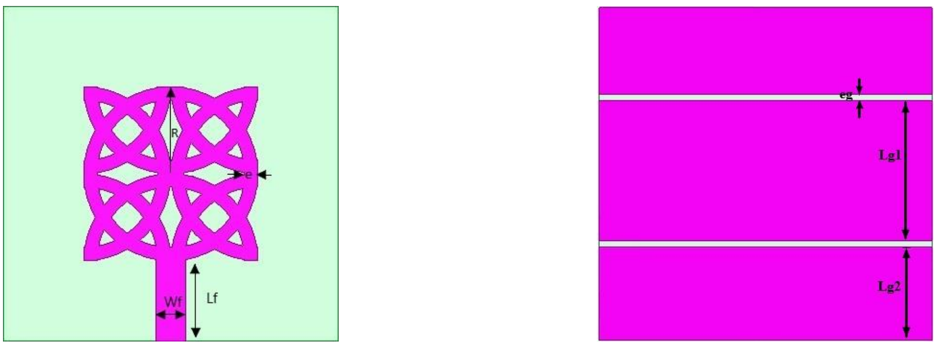

(a) (b)

Figure 1. Suggested patch geometry (a) top view and (b) bottom view

Figure 3 illustrates the antenna design process suggested by this letter. To design the initiator antenna shown in Figure 3(a) of radius R1, which operates at the resonant frequency of 2.48 GHz, we have adopted the simplest method, which is the transmission line, even if it presents less precise results. Balanis [20], Devi and Neog [21] describes this model in detail:

$$R1 = \frac{F}{\sqrt{1+\left(\frac{2h}{\pi \varepsilon_r F}\right)\left[ln\left(\frac{\pi F}{2h}\right)+1.7726\right]}} \quad (1)$$

where

$$F = \frac{8.791\times10^9}{f_r\sqrt{\varepsilon_r}} \quad (2)$$

After optimizing the initiator antenna dimensions, we get the size of 60×70×2 mm^3. The first iteration is presented in Figure 3(b), Figure 3(c) displays the second iteration, and the suggested patch is in Figure 3(d). The return losses of the initiator antenna as shown in Figure 3(a), the antenna with the first iteration as shown in Figure 3(b), the antenna with the second iteration as shown in Figure 3(b), and the suggested antenna as shown in Figure 3(d) are given in Figure 4.

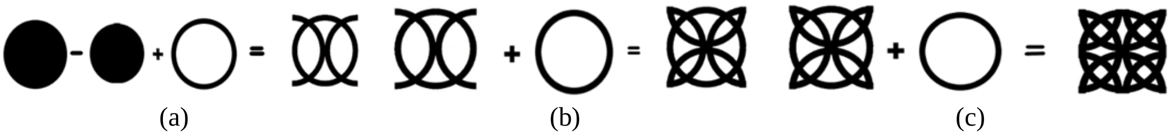

Figure 2. The proposed fractal antenna geometry steps configuration (a) first iteration, (b) second iteration, and (c) third iteration

Table 1. Proposed fractal antenna ultimate size

Settings	Values (mm)
W	50
L	50
Wf	4.5
Lf	12.19
R	1
E	2
Eg	1
Lg1	21
Lg2	14

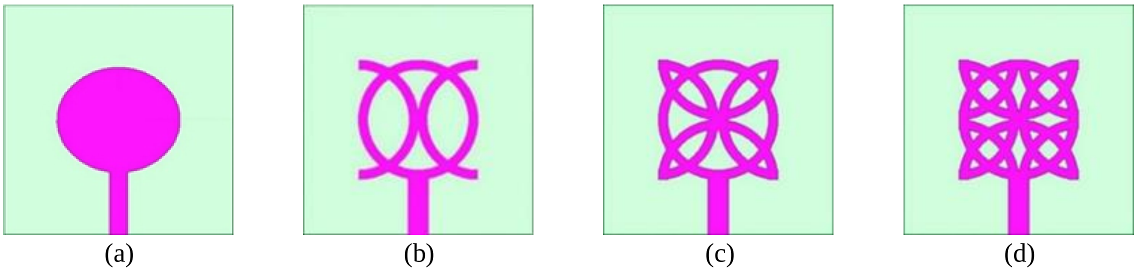

Figure 3. Suggested patch design steps (a) initiator, (b) first iteration, (c) second iteration, and (d) third iteration

Figure 4 shows that the initiator antenna returns losses can cover the frequency range 2.31-2.58 GHz with a return loss reaching -15.93 dB. For the first iteration, the antenna can cover the frequency range 2.11-2.51 GHz and 3.96-4.15 GHz with a return loss of -20.25 and -12.45 dB successively. Regarding the second iteration, the antenna may cover the three-band 2.40-2.73 GHz, 3.97-4.32 GHz, and 4.86-5.03 GHz with a return loss that varies between -13.96 and -23.54 dB. The suggested antenna can be operated in the frequency range 2.38-2.85 GHz, 3.90-4.35 GHz, and 5.12-5.33 GHz with a return loss that can reach -32.13 dB at the resonant frequency 5.23 GHz. The results of Figure 4 show that, in addition to the antenna size reduction, we have an increase in the number of resonant frequencies with an improvement in adaptation, and we have also increased the width of the bandwidth; this is due to the path of the surface current, which has become longer, and the proposed patch perimeter appears to be larger. We summarize the proposed fractal antenna process of changing the number of resonant frequencies, the operating frequency range, the resonating frequency, the return loss, and the gain in Table 2. According to Table 2, we note that we have also improved the gain that varies between 3.76 and 5.02 dB. This is due to the proposed antenna shape increasing the radiation intensity. With this increase in the number of operating ranges and gain, the proposed antenna can operate efficiently in WiMAX, WLAN, and C band applications.

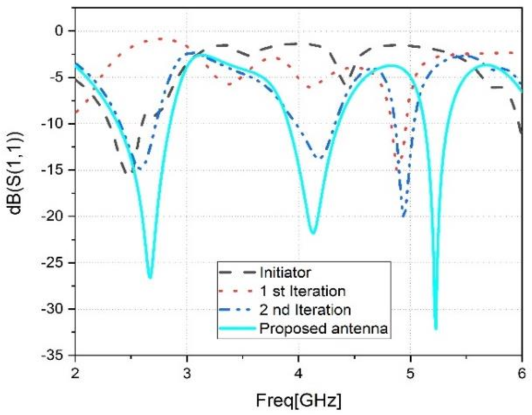

Figure 4. Simulated reflection coefficients result for initiator antenna at different iterations

Table 2. The increasing process of the resonances number, frequency ranges, resonating frequency, return loss, and gain

Iteration	Resonances Number	Frequency Ranges (GHz)	Resonating Frequency (GHz)	Return Loss (dB)	Gain (dB)
Initial antenna	1	(2.31-2.58)	2.49	-15.93	2.71
Antenna with the first iteration	2	(2.11-2.51)	2.29	-20.25	2.85
		(3.96-4.15)	4.03	-12.45	3.58
Antenna with the second iteration	3	(2.40-2.73)	2.57	-15.01	2.94
		(3.97-4.32)	4.18	-13.96	3.37
		(4.86-5.03)	4.94	-23.54	3.14
Antenna with thethird iteration	3	(2.38-2.85)	2.67	-26.62	3.76
		(3.90-4.35)	4.14	-21.76	4.06
		(5.12-5.33)	5.22	-32.13	5.02

The simulated voltage standing wave ratio (VSWR) depicted in Figure 5 is considered an important criterion in the study of antenna impedance matching. We can notice that the VSWR values of the proposed fractal antenna are less than 2 on all bandwidths; therefore, the antenna is suitably matched in impedance. The input impedance is shown in Figure 6. At the three bands, Figure 6 demonstrates that the input impedance agrees extremely well with the S11. Depending on the resonant frequency, the imaginary and real parts of the impedance vary.

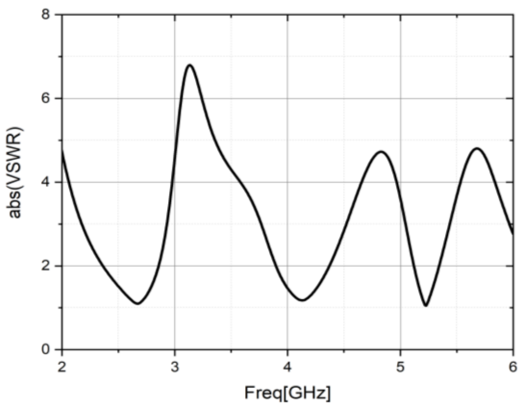

Figure 5. VSWR of the proposed antenna

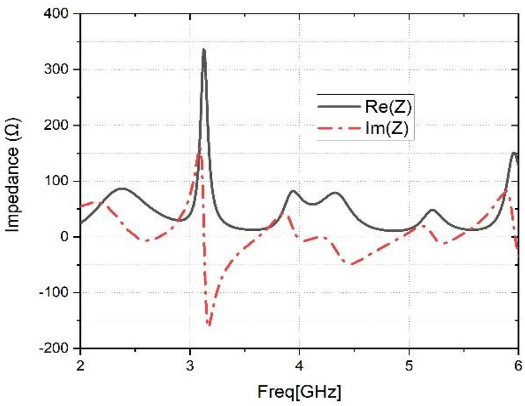

Figure 6. Antenna input impedance

The patch input impedance is affected by the surrounding environment, frequency, and geometry. We can correctly depict the input impedance by employing equivalent circuits using localized elements. The equivalent circuit of a broadband patch was calculated in the air by [22], [23]. The wideband antenna is considered as a multiband antenna, represented by N cells (each cell equivalent of parallel RLC circuits) in series with an inductance "L0" and a capacity "C0". The equivalent circuit is illustrated in Figure 7.

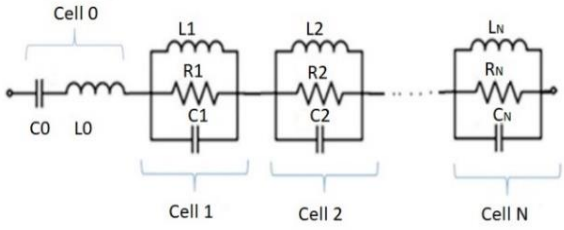

Figure 7. General topology of the patch equivalent circuit

The number of cells "N" corresponds to the number of resonant frequencies. We found three maximums in this study, which matched three cells (N=3). The diagram of the real part of the impedance is used to define the components (Li, Ri, Ci) of the cells (i=1, 2… N) of the equivalent circuit, and the diagram of the imaginary part is used to determine the input cell (C0, L0). In the air, [22], [23] describe the full steps for finding the antenna equivalent circuit. The equivalent circuit characteristics of the patch are shown in Table 3.

Table 3. Parameters of the patch equivalent circuit

Circuit Parameter	C0	L0	C1	L1	R1	C2	L2	R2	C3	L3	R3
Value	2.8 pF	0.27 nH	4.65 pF	0.96 nH	86.6 Ω	8.85 pF	0.29 nH	335 Ω	3.42 pF	0.47 nH	82.1 Ω

3. RESULTS AND DISCUSSION

To understand the operation and determine the characteristics of the proposed fractal antenna, we designed and simulated the antenna using the commercial Ansys HFSS electromagnetic (EM) wave simulator, and we checked the results using CST microwave studio software. We made the proposed antenna prototype. Afterward, we tested it using the vector network analyzer to prove the simulation results via the measured results. Figures 8(a) and 8(b) ilustrates the top view and bottom view of the manufactured antenna. The simulated and measured antenna return loss results are plotted in Figure 9.

(a) (b)

Figure 8. Antenna manufactured, (a) top view and (b) bottom view

Figure 9 shows that there is a small difference between the results of the simulated and measured reflection coefficient. For the second band, we have a very wideband in the measured results than in the simulated one, and for the third band, we have a small offset. This deviation is due to certain parameters, such as the manufacturing tolerance, the dielectric permittivity of the substrate, the simulation frequency width, the soldering conditions of the SubMiniature version A (SMA) connector, and the measurement circumstances. In order to have precise results of the reflection coefficient of the designed antenna, it is advisable to carefully manufacturing and measurement procedure, such as substrate quality, SMA, and welding precision. But in general, we can say that the simulated and measured results are in acceptable agreement. By observing the measured return losses results, we find a bandwidth of 0.31 GHz 2.46-2.77 GHz with the resonant frequency of 2.68 GHz. The second band has a bandwidth of 0.67 GHz 3.99-4.66 GHz where the resonant frequency equals 4.10 GHz, and the width of the third bandwidth is 0.19 GHz 5.24-5.43 GHz where the resonant frequency is 5.33 GHz. This result allows the proposed antenna to operate efficiently in Bluetooth, WiMAX, WLAN, LTE, and C-band applications. Table 4 summarizes the reflection coefficient results simulated and measured, and the commercial bands covered.

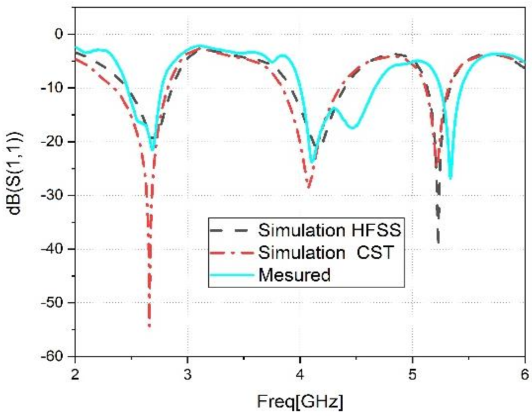

Figure 9. Results of reflection coefficients measured and simulated with CST and HFSS

Table 4. Simulated and measured bandwidth and frequency bands covered by the antenna

	Bandwidth (GHz)	Covered Commercial Bands
Simulation by HFSS	[2.46-2.86], [3.91-4.39], [5.13-5.33]	Bluetooth, WiMAX, WLAN, LTE, and C-band applications
Simulation by CST	[2.35-2.81], [3.84-4.36], [5.12-5.32]	
Measured	[2.46-2.77], [3.99-4.66], [5.24-5.43]	

Figure 10 illustrates the radiation patterns in the YZ plane and the XZ plane. Figure 10(a) illustrates the radiation pattern at the frequency 2.67 GHz, while at the frequency 4.14 GHz, it is shown in Figure 10(b), and that of the 5.23 GHz frequency, it is shown in Figure 10(c). We notice from the figure that in the XZ-plane, the radiation pattern at the resonant frequency of 2.67 GHz as shown in Figure 10(a) is omnidirectional and approximately omnidirectional in both other operating bands. Because when we increase in frequency, the FR-4 substrate experiences improper operation. Further, we notice that for the three operating bands, the radiation pattern in the YZ-plane has an “8” shape, which means that we have bidirectional radiation. As a result, it is clear that we have a monopoly-like radiation pattern.

To have an insightful understanding of the operation of the proposed fractal patch, we present in Figure 11 the surface current distributions simulated using Ansys HFSS at the three resonant frequencies. By analyzing Figure 11, we clearly notice that all parts of the suggested fractal patch are excited at the three resonant frequencies. Figure 11(a) depicts the current distribution of the 2.67 GHz resonant frequency. We note that the current flows largely in the center of the radiator and the feed line, which participates in a large part of the radiation in the first band. While the current is less dense in the parts of the radiator above the two slots of the ground plane, it helps to ameliorate the matching. By observing Figure 11(b), we notice that the current distribution is dominant in the area above the ground plane slits. So, they contributed to the second band. In addition, Figure 11(c) confirms that the distribution of current is distributed consistently throughout the radiator. Thus, we obtain the most adaptable band with a return loss equal to -32.13, and the highest gain which reaches 5.02 dB.

The comparison between our work and antennas in the literature for WLAN, Bluetooth, WIMAX, and LTE applications is presented in Table 5. It is clear from the table that the design of this patch is miniaturized with wide bandwidth and higher gain than most other antennas. These results allow the proposed antenna to cover with great efficiency the Bluetooth, WiMAX, WLAN, LTE, and C-band applications.

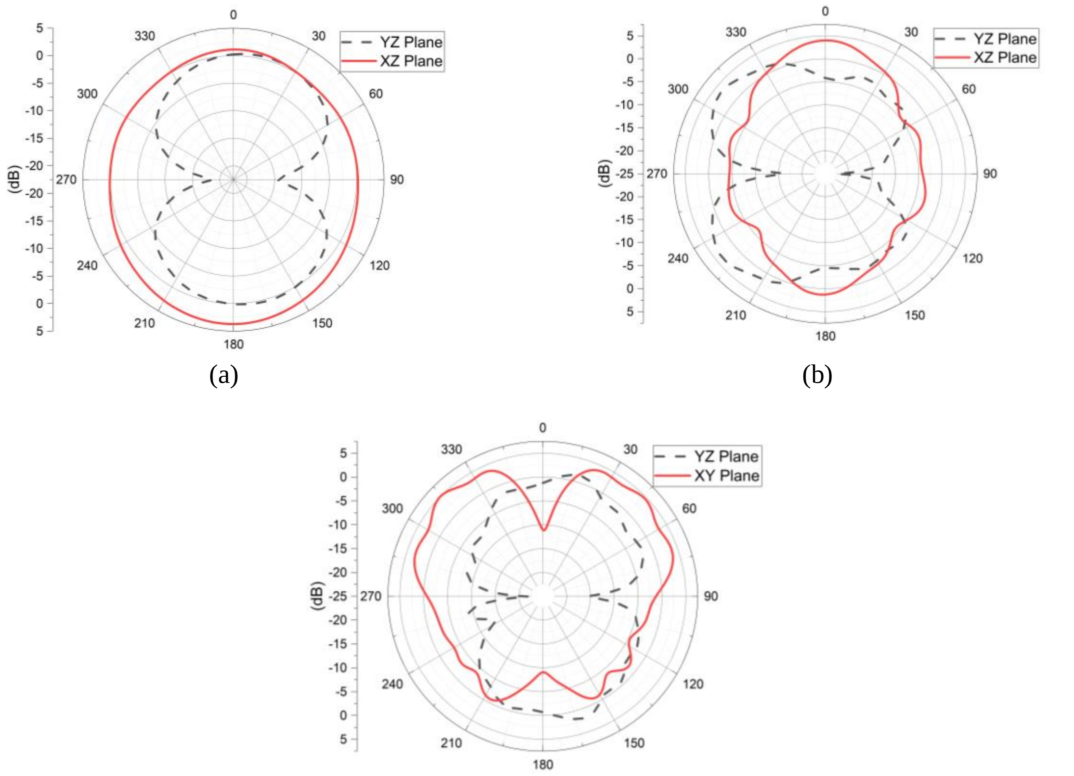

(a) (b) (c)

Figure 10. Radiation patterns in both plane XZ and YZ (a) 2.67 GHz, (b) 4.14 GHz, and (c) 5.23 GHz

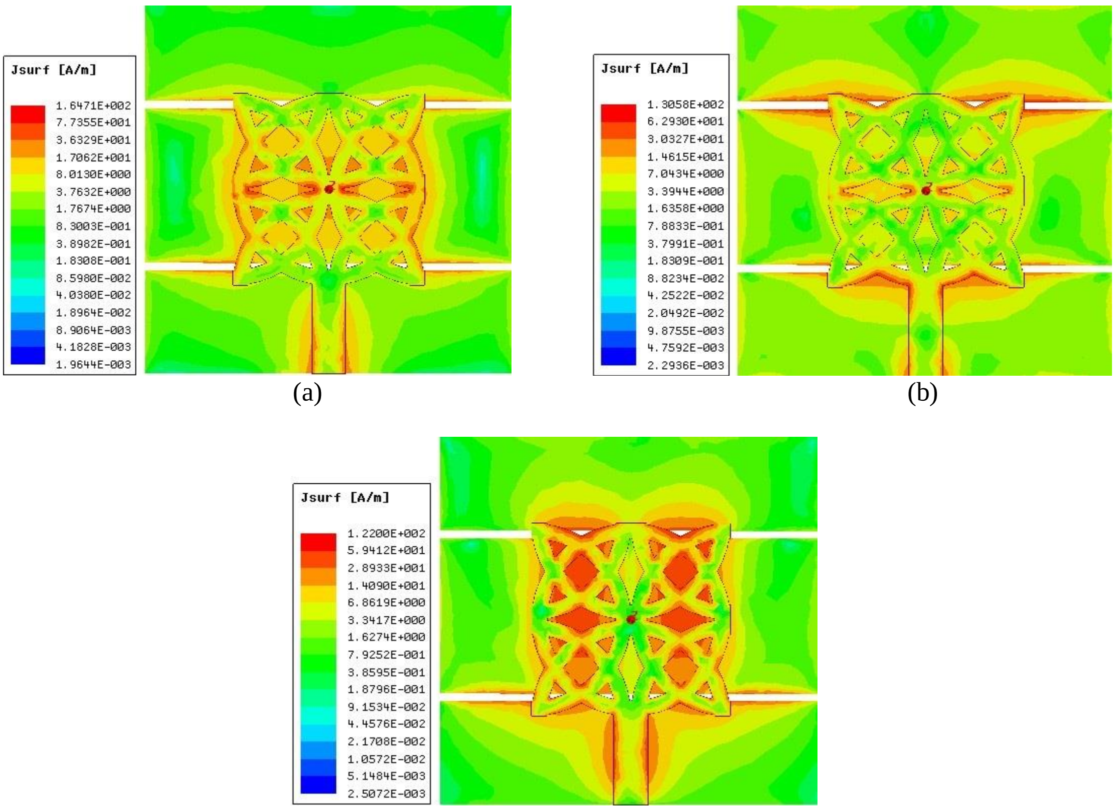

(a) (b) (c)

Figure 11. Surface current distributions (a) 2.67 GHz, (b) 4.14GHz, and (c) 5.23 GHz

Table 5. Comparison between this work and the works in literature

Ref.	Size (mm^3)	Bandwidth (GHz)	Gain (dB)
[24]	60×20×0.813	[2.4-2.48], [5.15-5.825]	1.63, 4.9
[8]	60×70×3	[0.780-960], [1.17-2.79]	1.69, 2.92
[25]	67×74×3.175	[2.45-2.57], [5.1-5.4]	6.15, 5.27
[26]	40×40×0.764	[3.28-3.51], [5.47-6.03]	0.6, 2.2
Our work	50×50×1.6	[2.46-2.77], [3.99-4.66], [5.24-5.43]	3.76, 4.06, 5.02

4. CONCLUSION

In this letter, a new circular fractal antenna with decreased dimensions and a simple structure is designed and manufactured on an FR4 substrate. In order to cover the Bluetooth, WiMAX, WLAN, LTE, and C-band operating bands. The results obtained by the measurement give bandwidths of 0.31 GHz 2.46-2.77 GHz, 0.67 GHz 3.99-4.66 GHz, and 0.19 GHz 5.24-5.43 GHz. By increasing in iteration, the number of resonance frequencies increases. However, the suggested patch exhibits good radiation characteristics and a high gain in the covered working bands. We conclude that the suggested antenna is very attractive and a suitable candidate for multiband applications.

REFERENCES

[1] I. H. Nejdi, Y. Rhazi, M. A. Lafkih, and S. Bri, "Designing multiband multilayered microstrip antenna for UMTS, ISM, communication satellite, HiperLAN and C-Band," in *2018 International Symposium on Advanced Electrical and Communication Technologies (ISAECT)*, Nov. 2018, pp. 1–8, doi: 10.1109/ISAECT.2018.8618728.

[2] F. Fertas, M. Challal, and K. Fertas, "Multi-L slots antenna for multiband applications," in *2019 International Conference on Advanced Electrical Engineering (ICAEE)*, Nov. 2019, pp. 1–5, doi: 10.1109/ICAEE47123.2019.9014757.

[3] K. Yu and X. Liu, "Design of tri-band antenna with rectangular ring for WLAN and WiMAX application," in *2017 Sixth Asia-Pacific Conference on Antennas and Propagation (APCAP)*, Oct. 2017, pp. 1–3, doi: 10.1109/APCAP.2017.8420552.

[4] I. H. Nejdi, "Frequency-reconfigurable multiband antenna based on pin switch for wireless applications," *Int. J. of Advanced Trends in Computer Science and Engineering*, vol. 9, no. 1.5, pp. 138–146, Sep. 2020, doi: 10.30534/ijatcse/2020/2091.52020.

[5] Y. Zhong, G.-M. Yang, and L.-R. Zhong, "Gain enhancement of bow-tie antenna using fractal wideband artificial magnetic conductor ground," *Electronics Letters*, vol. 51, no. 4, pp. 315–317, Feb. 2015, doi: 10.1049/el.2014.4017.

[6] P. S. Kirubavathy and K. Ramprakash, "Design of sierpinski fractal antenna for wideband applications," in *Int. Conf. on Innovations in Information, Embedded and Communication Systems (ICIIECS)*, 2017, pp. 1–4, doi: 10.1109/ICIIECS.2017.8276063.

[7] K. H. Kuther, I. H. Ali, and R. K. Ahmed, "Radiation effect of fractal sierpinski square patch antenna," *International Journal of Electrical and Computer Engineering (IJECE)*, vol. 10, no. 5, pp. 5329–5334, Oct. 2020, doi: 10.11591/ijece.v10i5.pp5329-5334.

[8] C. Ben Nsir, J.-M. Ribero, C. Boussetta, and A. Gharsallah, "A wide band transparent koch snowflake fractal antenna design for telecommunication applications," in *2019 IEEE 19th Mediterranean Microwave Symposium (MMS)*, Oct. 2019, pp. 1–3, doi: 10.1109/MMS48040.2019.9157327.

[9] N. S. M. Yaziz, M. K. A. Rahim, F. Zubir, N. S. Nadzir, R. Dewan, and H. A. Majid, "The improvement of first iteration log periodic fractal koch antenna with slot implementation," *International Journal of Electrical and Computer Engineering (IJECE)*, vol. 8, no. 4, pp. 2564–2570, Aug. 2018, doi: 10.11591/ijece.v8i4.pp2564-2570.

[10] Y.-W. Zhang *et al.*, "Simulation design of a broadband dual-polarized minkowski fractal microstrip antenna for S-Band," in *2018 IEEE International Symposium on Antennas and Propagation and USNC/URSI National Radio Science Meeting*, Jul. 2018, pp. 1087–1088, doi: 10.1109/APUSNCURSINRSM.2018.8609195.

[11] J. A. Russer, "Printed self-complementary Hilbert curve (SCHC) fractal broad-band antenna," in *2018 Baltic URSI Symposium (URSI)*, May 2018, pp. 206–209, doi: 10.23919/URSI.2018.8406743.

[12] S. K. Terlapu, J. Cheruku, and G. S. Raju, "On the notch band characteristics of koch fractal antenna for UWB applications," *International Journal of Control Theory and Applications*, vol. 10, no. 6, pp. 701–707, 2017.

[13] J. B. Benavides, R. A. Lituma, P. A. Chasi, and L. F. Guerrero, "A novel modified hexagonal shaped fractal antenna with multi band notch characteristics for UWB applications," in *2018 IEEE-APS Topical Conference on Antennas and Propagation in Wireless Communications (APWC)*, Sep. 2018, pp. 830–833, doi: 10.1109/APWC.2018.8503774.

[14] O. A. Safia and G. V Eleftheriades, "A new gosper island fractal UWB monopole antenna with enhanced bandwidth characteristics," in *2018 IEEE International Symposium on Antennas and Propagation and USNC/URSI National Radio Science Meeting*, Jul. 2018, pp. 1043–1044, doi: 10.1109/APUSNCURSINRSM.2018.8608404.

[15] J. Pourahmadazar, C. Ghobadi, J. Nourinia, and H. Shirzad, "Multiband ring fractal monopole antenna for mobile devices," *IEEE Antennas and Wireless Propagation Letters*, vol. 9, pp. 863–866, 2010, doi: 10.1109/LAWP.2010.2071372.

[16] P. Beigi and J. Nourinia, "A novel printed antenna with square spiral structure for WiMAX and WLAN applications," *Applied Computational Electromagnetics Society Journal*, vol. 30, no. 12, pp. 1329–1333, 2015.

[17] S. Verma and P. Kumar, "Compact arc-shaped antenna with binomial curved conductor-backed plane for multiband wireless applications," *IET Microwaves, Antennas and Propagation*, vol. 9, no. 4, pp. 351–359, 2015, doi: 10.1049/iet-map.2014.0427.

[18] P. Beigi, J. Nourinia, Y. Zehforoosh, and B. Mohammadi, "A compact novel CPW-fed antenna with square spiral-patch for multiband applications," *Microwave and Optical Technology Letters*, vol. 57, no. 1, pp. 111–115, 2015, doi: 10.1002/mop.28783.

[19] A. Zaidi, A. Baghdad, A. Ballouk, and A. Badri, "Design and optimization of a high gain multiband patch antenna for millimeter wave application," *International Journal of Electrical and Computer Engineering (IJECE)*, vol. 8, no. 5, pp. 2942–2950, Oct. 2018, doi: 10.11591/ijece.v8i5.pp2942-2950.

[20] C. A. Balanis, *Antenna theory: analysis and design*. 2016.

[21] R. Devi and D. K. Neog, "Determination of slot parameters of band-notched ultra wideband antenna using clonal selection algorithm," in *2014 Int. Conf. on Comput. Intell. n Commun. Netw*, Nov. 2014, pp. 60–63, doi: 10.1109/CICN.2014.25.

[22] I. Pele, A. Chousseaud, and S. Toutain, "Simultaneous modeling of impedance and radiation pattern antenna for UWB pulse modulation," in *IEEE Antennas and Propagation Society Symposium*, 2004, pp. 1871–1874, doi: 10.1109/APS.2004.1330566.

[23] M. Ansarizadeh, A. Ghorbani, and R. A. Abd-Alhameed, "An approach to equivalent circuit modeling of rectangular microstrip antennas," *Progress In Electromagnetics Research B*, vol. 8, pp. 77–86, 2008, doi: 10.2528/PIERB08050403.

[24] C. C. Hsu and H. H. Song, "Design, fabrication, and characterization of a Dual-BandElectrically small Meander-line monopole antenna for wireless communications," *Int. Journal of Electromagnetics and Applications*, vol. 3, no. 2, pp. 27–34, 2013.

[25] S. Panusa and M. Kumar, "Modified u-slot microstrip patch antenna with gain enhancement," Nov. 2014, doi: 10.1109/cicn.2014.30.

[26] A. Boukarkar, X. Q. Lin, and Y. Jiang, "A dual-band frequency-tunable magnetic dipole antenna for WiMAX/WLAN applications," *IEEE Antennas and Wireless Propagation Letters*, vol. 15, pp. 492–495, 2016, doi: 10.1109/LAWP.2015.2454001.

BIOGRAPHIES OF AUTHORS

Ibrahime Hassan Nejdi is State engineer in electronic and automatic systems engineering at the national school of applied science Tangier, Morocco, Ph.D. student at Faculty of Science and Technology, Sultan Moulay Slimane University, Morocco. He can be contacted at email: ibrahime.nejdi@usms.ma.

Rhazi Youssef was born in El jadida, Morocco, on June 01, 1982. He received the B. Sc. In Electrical Engineering from the University Ibn Tofail, Morocco in 2005. Received the (Ph.D.) degree from the University Moulay Slimane, Morocco, in 2019. Full Professor, University Moulay Slimane, Morocco. His current research interests include the full-wave analysis and microstrip patch antenna. He can be contacted at email: rhazi.lastid@gmail.com.

Mustapha Ait Lafkih received his PhD in Automatic Control from Cadi Ayyad University, Morocco, in 1993. He is currently a Professor of Automatics in the Electrical Engineering Department, Faculty of Sciences and Technology, Sultan Moulay Slimane University, Beni Mellal, Morocco. His research interests are in adaptive multivariable control. He can be contacted at email: aitlafkihmustapha@yahoo.fr.

Seddik Bri was a Professor in Electrical Engenrring Department, responsible of Material and Instrumenations group in High Scool of Technology, Moulay Ismail University, Meknes-Morocco. His recharch interested in commincations systems and publisched 3 International Patents (PCT), 8 National Patents, 150 Publications, 160 Internatioanls conferences, 10 Books and 9 chapters. He can be contacted at email: briseddik@gmail.com.

Mohammed Lamsalli was born in Kenitra, Morocco, in 1980. He received his License degree in 2006 from the University Ibn Tofail, Kenitra, Morocco. In 2010 he took his Master's degree and (Ph.D 2019) in electronics and telecommunications from the University Abdelmalek Essaadi, Tetouan, Morocco. His current research interests include the optimization technique of passive and active microwave structures (antennas, filter) using genetic algorithms. He can be contacted at email: lamsalli.mohammed@gmail.com. Web of science researcher ID: ABG-8151-2021.